A Spherical Slot Array Applicator for Medical Applications

Monai Krairiksh, Toshio Wakabayashi, *Member, IEEE*, and Wiwat Kiranon

***Abstract*—A new type of microwave hyperthermia applicator is proposed and analyzed. A cavity, consists of concentric conducting partial spheres which are enclosed by a part of a conducting cone, is employed to excite an array of slots coherently. From numerical results that we obtained, it is possible to focus the electric field radiated from the slots to the center of the sphere where a tumor is assumed to be located. Furthermore, SAR distributions of some applicators are obtained by using computer, and these applicators have been designed. From the measured results of electric field distributions at 2450 MHz, it is found that the focusing characteristics are achievable. Thermographic studies show that the heating volume can be varied by using different number of slots and the maximum heating depth is 3 cm.**

I. Introduction

A MICROWAVE applicator that can perform selective heating plays an important role in a non-invasive hyperthermia cancer treatment. It is employed, without invading into a human body, to apply electric field to elevate temperature of the tumor to a hyperthermic range while maintaining the surrounding healthy tissue undamaged. A field penetration depth into the body is inversely proportional to the operating frequency. Using low frequency makes the applicator beamwidth wide at the expense of ineveitably large size. To perform selective heating to obtain a small hotspot size, an array of applicators may be utilized. The size of an applicator becomes smaller when the operating frequency is in a microwave range.

Several types of non-invasive applicator have been investigated in literatures [1]–[7]. All of them correspond to a kind of a single applicator which are light in weight, simple structure and compact. However they possess a disadvantage that they have no focusing ability, then significant areas of healthy tissue adjacent to the tumor are often heated. The articles in [8]–[10] introduce that the absorbed power distribution pattern can be modified by arranging the applicators in array. The use of an array of two microstrip applicators of which the field dirtribution can be controlled by varying an angle between them had been investigated by James *et al.* [11]. The structure of the array is unfortunately complicated because it needs an external power divider and phase shifter. Lens type applicators have been developed by Nikawa *et al.* [12]–[14]. These types of applicators including the one developed by Guy *et al.* [15] are suitable for a part of the human body that has a cylindrical shape. For some parts of human body such as breast and head which are closely spherical in shape, the authors [16], [17] have proposed an applicator with a rather proper shape and some results have been reported.

In this paper, microwave applicators made of spherical slot array are proposed and analyzed. Calculations are carried out at a frequency of 2450 MHz to investigate the appropriate applicator size for focusing electric field deepen into a human muscle. Experimental results of electric field distribution coincides with the analytical results. The focusing ability can be controlled by varying the number of slots. Since in the proposed applicator structure, the power divider and the phase shifter are integrated together, it makes the applicator structure become light weight, rugged, compact and easy to handle. The unique feature of this applicator is the capability not only to conform to the spherical part of the human body, but also applicable to the planar part of the body. The applicator has a remarkable characteristic that it can perform selective heating with maximum heating depth of 3 cm at the testing frequency.

II. Analysis and Design

A. Slot Array Applicator

The proposed hyperthermia applicator is composed of a concentric spherical cavity as shown in Fig. 1(a), which is used to excite an n-slot array as radiators. The cavity is excited in TM_{mn} mode by a coaxial cable with the inner conductor protrudes into it. The inner and outer spherical radii of the cavity are a and b as shown in Fig. 1(b). Both spherical conductors are enclosed by a conical conductor at an angle $\theta = \theta_c$. The slot radiators are cut on the inner spherical conducting surface along the line with angle $\theta = \theta_o$, along which the surface current density is predicted to be maximum. In Fig. 1(c), ϕ_{oi}'s are supposed to be the center of the ith slot $(i = 1, 2, \cdots, n)$. To produce a focused field at a point in a medium, the field contributions from each radiator should be inphase at that point, then, to obtain a focus of the fields from every slot radiator at the center of the sphere, the following condition must be held

$$\frac{2\pi a}{\lambda} + \psi_p = \text{constant} \tag{1}$$

where λ is the wavelength of fields in the medium, and ψ_p $(p = 1, 2, \cdots, n)$ denotes phase of excitation fields at the slots.

It is evident from (1) that ψ_p should be identical, namely, each slot has to be inphase excited. Fortunately it is possible

Manuscript received September 14, 1993; revised February 22, 1994.

M. Krairiksh and W. Kiranon are with the Faculty of Engineering, King Mongkut's Institute of Technology, Ladkrabang, Bangkok 10520, Thailand.

T. Wakabayashi is with the School of Engineering, Tokai University, Hiratsuka, Kanagawa 259-12, Japan.

IEEE Log Number 9406824

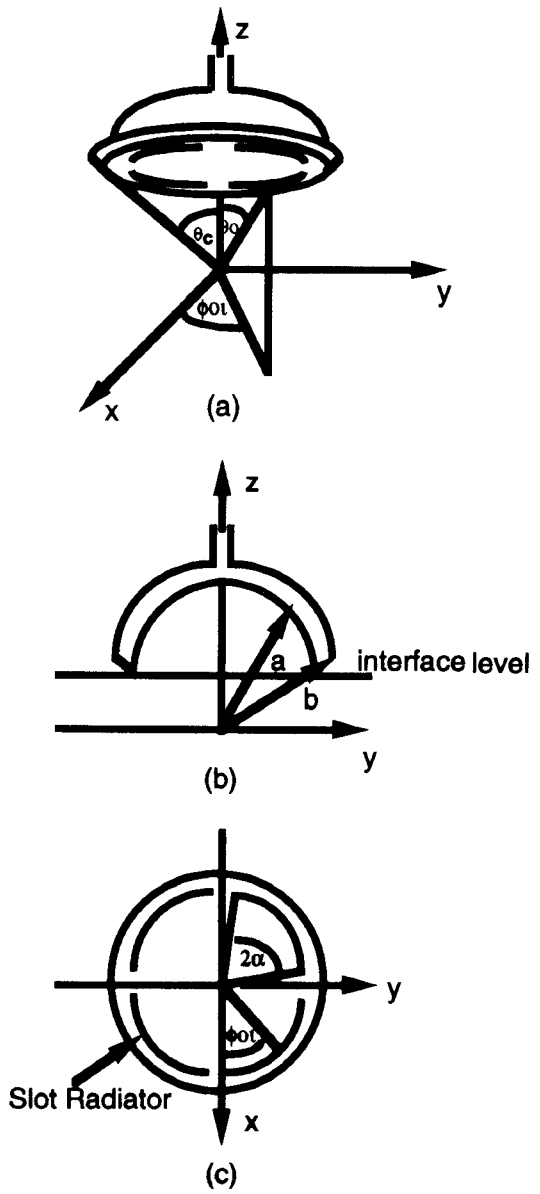

Fig. 1. Geometry of a spherical slot array applicator (a) Perspective view (b) Side view (c) Bottom view.

to force the field strength inside the cavity to be the function that is independent from the azimuthal angle ϕ, and this means every slot radiator can be excited by equal field strength. It can be accomplished by exciting the cavity in TM_{on} mode [18]. The inner radius a and outer radius b of the cavity must be satisfied by the following relation

$$\frac{j_n'(\beta a)}{n_n'(\beta a)} = \frac{j_n'(\beta b)}{n_n'(\beta b)} \tag{2}$$

whereas the conical angle θ_c must satisfy the relation

$$P_n^o(\cos\theta)|_{\theta=\theta_c} = 0 \tag{3}$$

where, $P_n^o(\cdot)$ denotes an associated Legendre function of degree n order o, $j_n'(\cdot)$ and $n_n'(\cdot)$ are the derivative of spherical Bessel's function of the first and second kind repectively, β is a phase constant of wave inside the cavity.

When operating frequency is specified, β can be determined. Then the spherical radii and the conical angle θ_c from (2) and (3) can be found. The contour of constant θ_o where the surface current density is maximum can be found by maximizing $P_n^o(\cos\theta)$ with respect to θ:

$$\theta_o | \max_{\theta} P_n^o(\cos\theta) \tag{4}$$

Recalling that the field has the same phase at the same conical angle θ [18], the slots are to be cut horizontally along an azimuthal plane of the sphere at the positions of the same angle θ_o so as to produce inphase excitation to each radiator. It is evident that the total length of the slots are limited by the circumference of the sphere at the conical angle θ_o minus the spacings between the slots. For the sake of field expressions, a slot length is expressed as a function of angle α as shown in Fig. 1(c).

B. Electric Field Distribution and Specific Absorption Rate

An outstanding performance of a hyperthermia applicator is its capability that can deposit the energy of electromagnetic field to produce a hotspot. The details about the position and size of the hotspot can be revealed by investigation about electric field distribution and Specific Absorption Rate (SAR). SAR is the quantity that is defined by the derivative of the incremental energy absorbed by an incremental mass contained in a volume element [9]. It is related to the temperature rise of heating material by

$$\text{SAR} = 4184c(dT/dt) \quad (\text{W/kg}) \tag{5}$$

where $c = 0.86$ (kcal/kg °C) is the muscle phantom specific heat, T is temperature (°C) and t is time (second). SAR is also expressed as

$$\text{SAR} = (0.5\sigma/\rho)|\mathbf{E}_T|^2 \quad (\text{W/kg}) \tag{6}$$

where σ and ρ are the conductivity (S/m) and density (gm/cc) of the medium, respectively and $\mathbf{E}_T$ is the resultant electric field induced in the heating material.

Generally the electric field distribution at the aperture of each slot can be expressed in series of terms of orthogonal set of arbitrary field distribution by a Fourier expansion. However, for a narrow slot at which the field distribution can be recognized as transverses, all field to the slot can be represented in terms of sinusoidal distribution with zero field at the end of the slot. Therefore, the aperture electric field distribution of the slot can be expressed as the following

$$\begin{aligned}\mathbf{E}_a(a,\theta,\phi) = {} & \mathbf{a}_r B_{mn}[\mathbf{N}_{mn}(a,\theta,\phi)] \\ & + \mathbf{a}_\theta(1/a)\delta(\theta-\theta_o) \\ & \cdot \cos[\pi(\phi-\phi_o)/2\alpha], \\ & \phi_{oi} - \alpha \le \phi \le \phi_{oi} + \alpha \\ = {} & 0 \qquad \text{elsewhere}\end{aligned} \tag{7}$$

where $\mathbf{a}_r$ and $\mathbf{a}_\theta$ denote unit vectors r and θ directions, respectively, and δ is the delta function. Also $\mathbf{N}_{mn}$ is a vector spherical harmonics and B_{mn} is a coefficient.

TABLE I
THEORETICAL PERFORMANCE OF TWO-SLOT APPLICATORS

mode	a (cm)	b (cm)	$\theta_c(^\circ)$	$\theta_o(^\circ)$	$2\alpha(^\circ)$	Penetration Depth from the Interface (cm)	EFS of the Desired Hotspot (cm^2)
TM_{01}	2.18	3.47	90.0	90.0	178	0.5	0.4
TM_{02}	4.30	5.30	54.5	45.0	178	2.7	1.0
TM_{03}	6.23	7.31	39.6	31.0	178	0.4	—

The electromagnetic field maintained by the slot aperture field at any point in space can be expressed in terms of vector spherical harmonics [19]. Thus the near-zone electric field of the slot can be written as

$$\mathbf{E}(r,\theta,\phi) = \sum_{n=0}^{\infty}\sum_{m=-n}^{n}[A_{mn}\mathbf{M}_{mn}(r,\theta,\phi) + B_{mn}\mathbf{N}_{mn}(r,\theta,\phi)] \tag{8}$$

where the vector spherical harmonics $\mathbf{M}_{mn}$ and $\mathbf{N}_{mn}$ are given as

$$\mathbf{M}_{mn}(r,\theta,\phi) = \mathbf{a}_\theta[h_n^{(1)}(kr)(jm/\sin\theta)P_n^m(\cos\theta)e^{jm\phi}] + \mathbf{a}_\phi\{h_n^{(1)}(kr)[P_n^m(\cos\theta)]'e^{jm\phi}\} \tag{9}$$

and

$$\begin{aligned}\mathbf{N}_{mn}(r,\theta,\phi) &= \mathbf{a}_r\{(1/kr)h_n^{(1)}(kr)n(n+1)P_n^m(\cos\theta)e^{jm\phi}\} \\ &+ \mathbf{a}_\theta\{(1/kr)[rh_n^{(1)}(kr)]'[P_n^m(\cos\theta)]'e^{jm\phi}\} \\ &+ \mathbf{a}_\phi\{(1/kr)[rh_n^{(1)}(kr)]'(jm/\sin\theta) \\ &\cdot P_n^m(\cos\theta)e^{jm\phi}\}\end{aligned} \tag{10}$$

If the electric field $E(a,\theta,\phi)$ given in (8) is matched to the slot aperture field $E_a(a,\theta,\phi)$ given in (7), the coeffients A_{mn} and B_{mn} can be determined as follows

$$A_{mn} = \frac{-jm\alpha P_n^m(\cos\theta_o)\cos(m\alpha)\cos(m\phi_o)}{a(\pi^2-4m^2\alpha^2)(1+\delta_m)n(n+1)} \cdot \int_0^{\theta_c}[P_n^m(\cos\theta)]^2\sin\theta\,d\theta \tag{11}$$

and where,

$$\delta_m\begin{cases}=1, & m=0\\ =0, & m\neq 0\end{cases}$$

and

$h_n^{(1)}(\cdot)$: spherical Hankel function of the first kind,
$k = \omega\sqrt{(\mu_o\epsilon)(1-j\sigma/\omega\epsilon)}$.

Once A_{mn} and B_{mn} are obtained, the near-zone electric field of slot is completely determined.

Since propagation medium under investigation is lossy, it is assumed that E_θ at θ greater than E_θ at θ_c vanishes and mutual coupling is negligible. Integration in (11) and (12), shown at the bottom of the page, can be numerically accomplished.

The resultant electric field is calculated by summing up the the field from each slot. That is

$$\mathbf{E}_T = \sum_{i=1}^{n} E_i \tag{13}$$

$\mathbf{E}_T$ is the total electric field from the slot array and $\mathbf{E}_i$ ($i = 1,2,\cdots n$) is the electric field from the ith slot. Substituting $\mathbf{E}_T$ in (13) into (6) the SAR can be calculated.

III. NUMERICAL RESULTS

An applicator of a slot array can be designed to operate in several modes (TM_{on}). Each of them has different characteristic and dimensions. It is essential to consider about an acceptable size of the cavity to be an excitor. The dimensions of the two-slot applicators excited by three modes TM_{01}, TM_{02} and TM_{03} be obtained from (2)–(4) at 2450 MHz, and are shown in Table I.

By computer simulations, SAR distributions of these applicators are shown in Fig. 2. It is noted that the maximum of SAR appears near the slot surfaces and decreases along the path out of the slots. The penetration depth is defined by a depth at which SAR reduces to 13.5% [9]. The effective field size (EFS), the area that the temperature rise is half of the maximum temperature, is defined by a 50% SAR contour [21]. Fig. 2(a) illustrates that an applicator made from a TM_01 cavity can focus an electric field at the center of the spherical cavity. The EFS of the desired hotspot is approximately 0.4 cm^2.

$$B_{mn} = \frac{\pi\alpha\cos(m\alpha)\cos(m\phi_o)}{ka^2(\pi^2-4m^2\alpha^2)n(n+1)}\int_0^{\theta_c}[P_n^m(\cos\theta_0)]^2\sin\theta\,d\theta \cdot \frac{[P_n^m(\cos\theta_o)]'\sin\theta_o[ah_n^{(1)}(ka)]'}{[\{(1+\delta_m)\pi/2(2n+1)\}\{(n+1)[h_{n-1}^{(1)}(ka)]^2+n[h_{n+1}^{(1)}(ka)]^2\}+n(n+1)\alpha[h_n^{(1)}(ka)/ka]^2]} \tag{12}$$

TABLE II
DESIGN DATA AND EXPERIMENTAL PERFORMANCE OF TM_{02} MODE APPLICATOR WITH DIFFERENT NUMBER OF SLOTS

Number of Slots	2	3	4
a (cm)	4.3	4.3	4.3
b (cm)	5.3	5.3	5.3
$\theta_c(^\circ)$	54.5	54.5	54.5
$\theta_0(^\circ)$	45	45	45
$\phi_{0z}(^\circ)$	0, 180	0, 120, 240	0,90, 180, 270
slot length (cm)	9.25	6.0	4.5
penetration depth from the interface (cm)	1.9	3.0	2.9
EFS of the desired hotspot (cm^2)	5.1	7.7	13.8
net power for 235 W/kg (W)	111	98	93

However for an applicator made of a TM_{02} cavity which has an inner spherical radius 4.3 cm, the center of the sphere is at the depth of 2.5 cm from the horizontal interface level as shown in Fig. 2(b). It is found that in this case the EFS is around 1 cm^2, which is desireable for a local heating because heat can be confined in a remarkably small area. It can heat a tumor without burning surrounding healthy tissue. By contrast from the SAR distribution of an applicator made of a TM_{03} cavity in Fig. 2(c), focusing capability is not noticable. Therefore, it is concluded that in order to focus electric field deep into a lossy material such as human muscle, a TM_{02} cavity is the most suitable to feed the slot array. However for a specified applicator, it is interesting to consider the number of slots that should be utilized in order to confine an EFS of the desirable hotspot suited to a tumor size.

Fig. 3 shows the squared electric field distribution computed on the focal plane of the applicators with a TM_{02} cavity. From the results, we can determine the EFS. The dimensions of these applicators are shown in Table II. It is observed that the -3 dB beamwidth which correspond to the EFS of the two-slot applicator is 1.1 cm on the x-axis and 1.2 cm on the y-axis. For the three-slot applicator the EFS is a little bit larger than the case of the two-slot, and the peak amplitude is 1.5 dB higher than that of the two-slot one. Moreover for the four-slot applicator, the -3 dB beamwidth is 1.9 cm in both x and y directions with the peak amplitude of 2.5 dB higher than the two-slot applicator. This implies that the EFS can be controlled by using different number of slots.

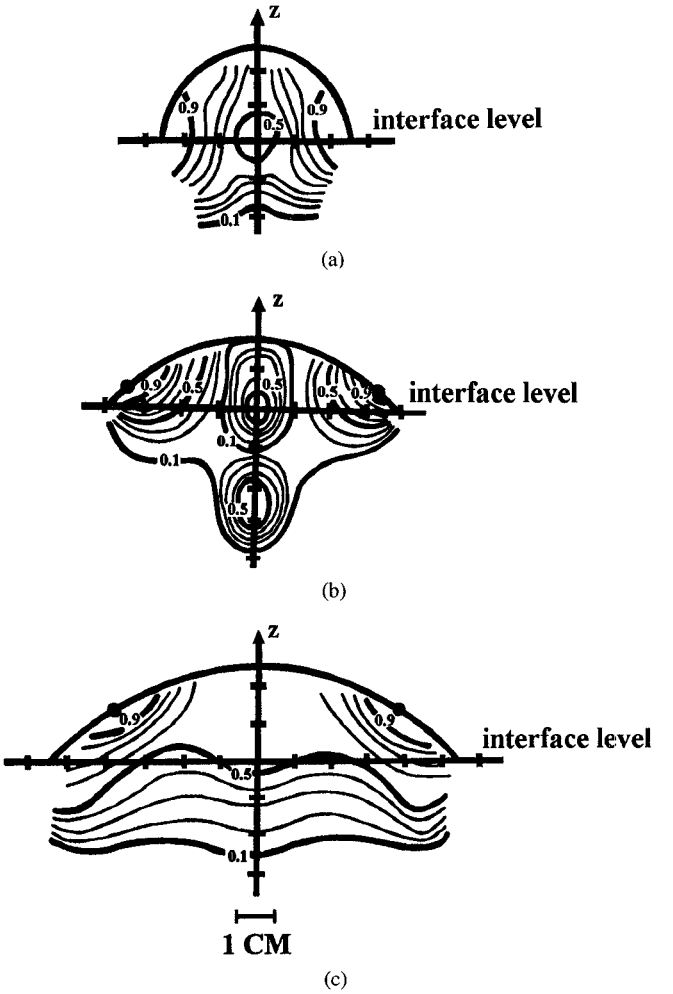

Fig. 2. Calculated SAR distribution on x–z plane of applicators excited by three different cavity mode for a human muscle ($\epsilon_r = 49.6 - j16.5, \sigma = 2.2$ S/m, and $\theta = 1.0$ gm/cc). (a) TM_{01}. (b) TM_{02}. (c) TM_{03} • slot location.

IV. PERFORMANCE OF APPLICATORS

A. Radiation Patterns

A particular clinical requirement for which the spherical applicator may be suitably applicable is to locally heat a tumor in the spherical part of human body such as breast or head, etc. Fig. 4 shows the field mapping system [22] to measure radiation patterns of the applicators; one-slot and two-slot applicators. In this figure the water tank with a spherical bottom is placed on the surface of the applicator. The inner and outer radii of the cavities of the applicators are 4.3 cm and 5.3 cm, respectively. The slot location is in the direction of $\theta_o = 45^\circ$. Since the circumference of the sphere at such angle is 19.0 cm, the slot length of 9.25 cm is chosen and the spacing between the slots is 2.5 mm for two-slot applicator. The photograph of the two-slot and three-slot array applicators which were designed to operate at 2450 MHz with radii a and b are 4.3 and 5.3 cm respectively and θ_c is 54.5° is shown in Fig. 5. A 3.5 mm long electric field probe was moved on the x–z plane to measure the distribution of squared electric field

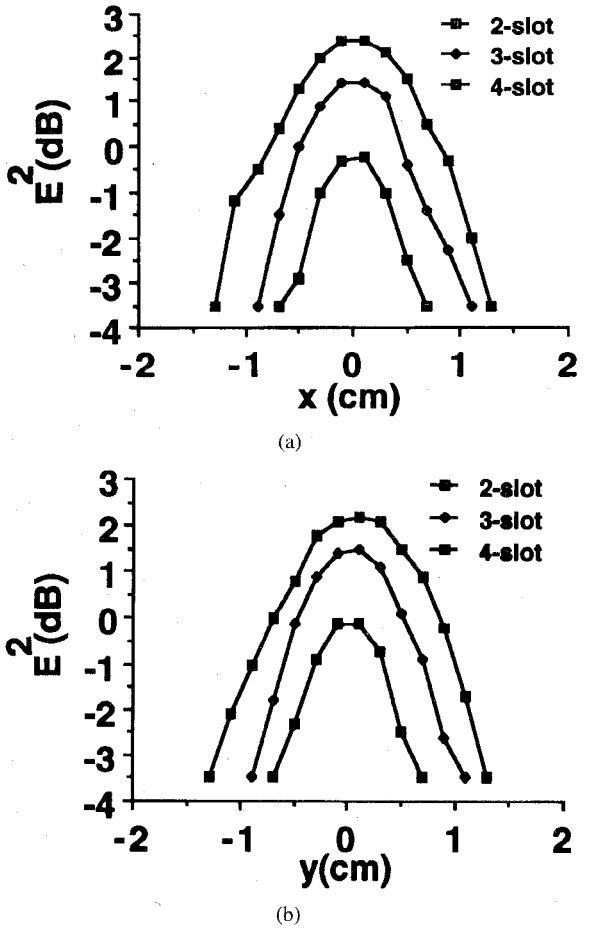

Fig. 3. Simulation of squared electric field distribution on the focal ($x-y$) plane. It is normalized to the field at the origin from the two-slot applicator. (a) on x-axis, (b) on y-axis.

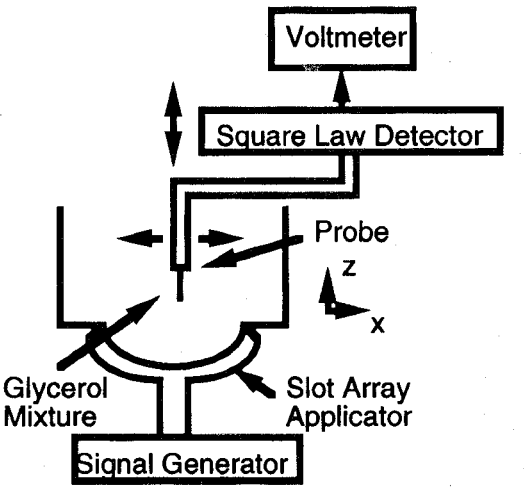

Fig. 4. Field mapping system.

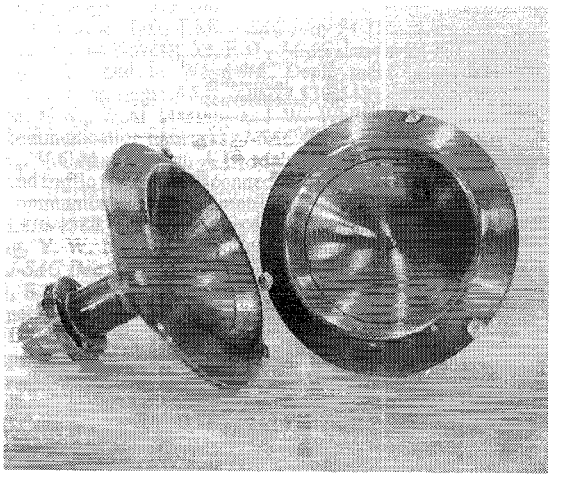

(a) (b)

Fig. 5. Photographs of a two-slot applicator, $a = 4.3$ cm, $b = 5.3$ cm, $\theta_c = 54.5°, \theta_0 = 45°$. (a) Two-slot applicator: slot length = 9.25 cm. (b) Three-slot applicator: slot length = 6.0 cm.

intensity in phantom simulating human muscle prepared from glycerol and water (30:70 by weight). Field patterns which are measured on $x-z$ plane are shown in Fig. 6. For the one-slot applicator, it is seen that the square of electric field intensity has its maximum at the slot and its amplitude decreases along the distance. A contour of -8.68 dB which correspond to a penetration depth (SAR = 13.5%) is around the center of the sphere which is 2.5 cm from the interface level. For the two-slot applicator, the contour of -6 dB passes the center and the energy is 2 dB higher than that of the one-slot applicator. It is observed that there is an additional hotspot around the center. The spotsize is defined as the area surrounded by a -3 dB contour down from the value at the center (-9 dB contour). The hotspot appears deep inside the heating material in addition to the two spots near the slots. The width of this spot is about 1 cm. A field pattern of the three-slot applicator is illustrated in Fig. 6(c). The desirable hotspot at the center is remarkable. The maximum value at the center is around -3 dB and the hotspot size (-6 dB) is almost the same as that of the two-slot applicator. However, the penetration depth is longer. From this investigation it is realized that an appropriate cooling water bolus must be designed to cool down the heat near the surface and its shape should be a spherical shape which conforms to the surface of the applicator. The material filled in the bolus should be the cold low loss material with dielectric constant which is close to that of the human muscle in order to maintain the field matching condition.

B. Input Impedance

An input impedance is an important parameter associated with power transmission from a source via an applicator to a material to be heated. Therefore, an input impedance of an applicator must be examined when it is attached to a muscle phantom. Experiments were made by using an HP 8720C Microwave Network Analyzer to measure an impedance of three applicators as shown in Table II. The results are plotted on the Smith Chart as shown in Fig. 7. When these three applicators directly contact the human muscle phantom of which dielectric constant is 48 [22], it is found in Fig. 7 that the two-slot applicator has an impedance with high mismatch. Its impedance rotates on a smith chart from an inductive impedance at 2.0 GHz and becomes a capacitive impedance at 3.0 GHz. For the three-slot applicator, the impedance changes from an inductive at 2.0 GHz and becomes capacitive at 3.0 GHz. At the operating frequency, its impedance is inductive

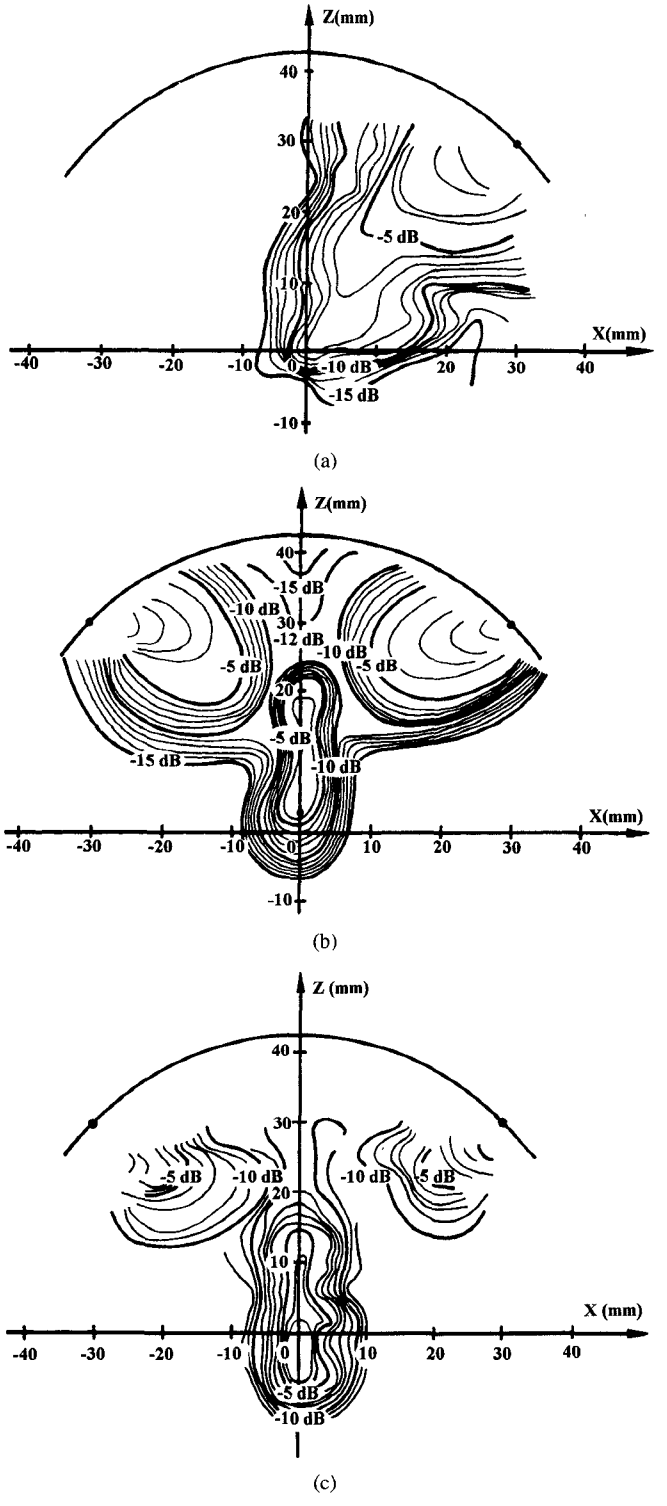

Fig. 6. Field pattern on the x–z plane plotted relative to the maximum value which occurs at the slot aperture. (a) One-slot applicator. (b) Two-slot applicator. (c) Three-slot applicator.

with lower mismatch. The four-slot applicator behaves as an inductive impedance at the lower portion of the testing frequency and becomes a capacitive impedance at the higher frequency. The impedance at the operating frequency is capacitive and is the closest one to 50 ohms.The VSWR of the two-slot, three-slot and four-slot applicators are 3.35, 2.16 and 1.13, respectively. Also their reflection coefficient are 0.54, 0.4 and 0.05, respectively. When these applicators are in direct

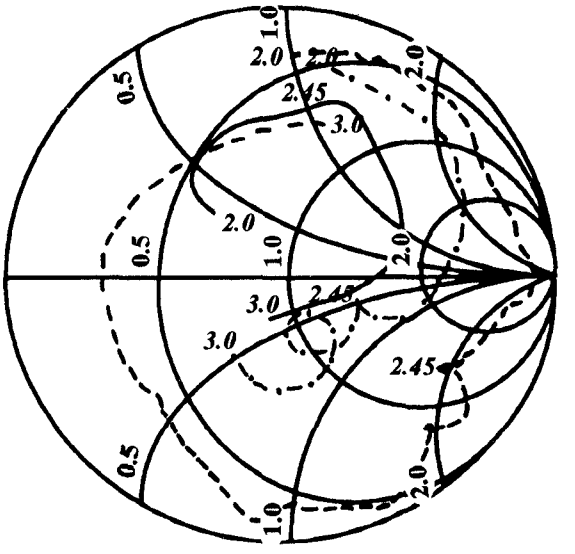

Fig. 7. Input impedance for applicators in direct contact with simulated muscle phantom two-slot applicator: — — — —; three-slot applicator: ——; and four-slot applicator: — · — · —.

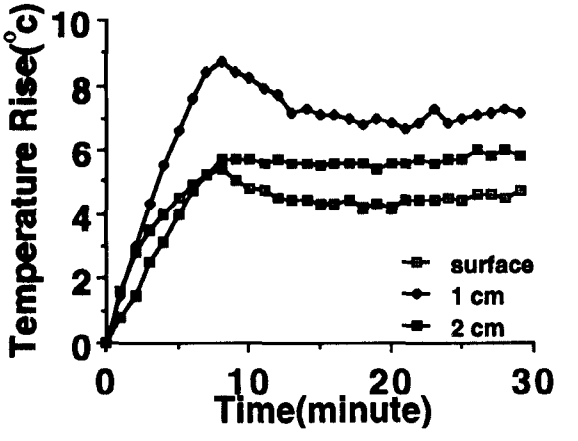

Fig. 8. Temperature-time relationships of the three-slot applicator measured at three different depths (surface, 1 cm and 2 cm). Net input power is kept at 42 W at the first eight minutes then it is reduced to 17 W.

contact with a planar phantom, the VSWR are drastically increased due to the fact that there is a free space region between the applicator and a phantom surface. Consequently in application with planar structure a water bolus must be designed so that its shape is the same as the free space area between the applicator and the heating material. This bolus will not only behave as a cooling system of the surface but also as a field matching device.

C. Temperature-Time Relationship

In hyperthermia application it is desirable to elevate the tumor temperature up to a hyperthermic range (42°–45°C). It means that the temperature rise in the tumor is in the range of 5°–8°C higher than the normal temperature of a human body (37°C). In addition the rate of temperature rise should be kept around 1°C/min so as not to injure the patient. An experiment was performed to get the information to design a hyperthermia system that satisfied such requirements. In the experiments, a planar human muscle phantom and a three-slot applicator with a 4 mm thick water bolus were prepared.

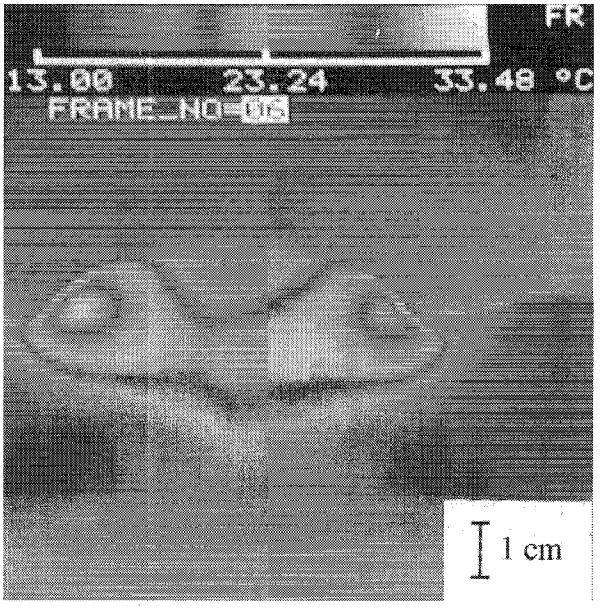

(a)

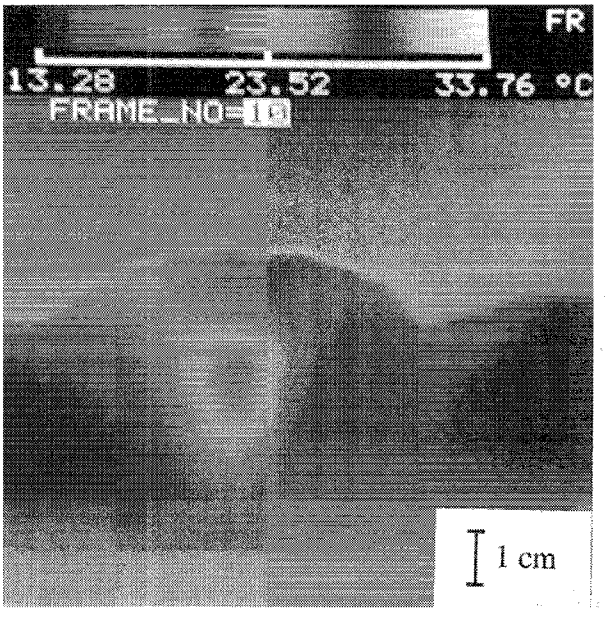

(b)

Fig. 9. Heating pattern of a two-slot applicator in a spherical phantom. (a) Without bolus. (b) With bolus.

The water temperature is 22°C with the flowrate of 0.5 l/min. In order to elevate the temperature at the depth of 2 cm up to 6°C with the rate of about 1°C/min, a net power of 42 W was applied to the applicator for first 8 minutes. Then, the power was reduced to 17 W to retain the constant temperature. Temperature at three points i.e. at the surface, 1 cm and 2 cm depth along the central region of the applicator were measured using the fiber thermometers. From the experimental results, it is found that the rate of temperature rise ΔT are shown in Fig. 8, temperature rise at the surface is 1.25°C/min in the first 2 minutes, and then it falls down due to thermal diffusion in cooling water. It is expected that the surface temperature can be lowered if the water temperature is decreased. For the depth of 1 cm, temperature rise is around 1.25° C/min in the first 8 minutes. The maximum temperature rise at this depth is in excess of 9°C which is 1°C higher than the hyperthermic range. This problem can be solved by controlling bolus temperature and the power. It is seen that this three-slot applicator is useful for hyperthermia.

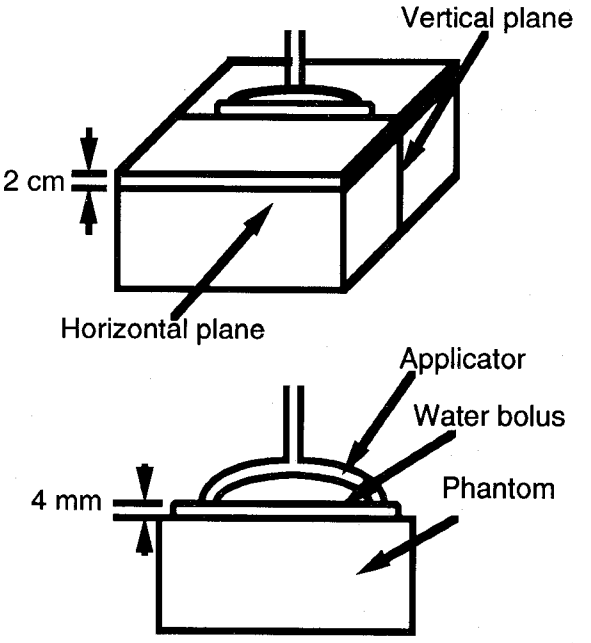

Fig. 10. Dimensions of the flat phantom and water bolus including the measuring plane.

D. Heating Patterns

The muscle equivalent phantom is composed of 0.4% NaCl, 0.02% NaN_3 and 4% Agar. The experiments were performed to illustrate the focusing effect in spherical phantom and to evaluate hotspot size in planar phantom. The two-slot applicator as mentioned in the previous section were employed to heat a spherical phantom with a radius of 4.3 cm. Fig. 9(a) shows a heating pattern on x–z plane after 85 W net power, (incident power-reflected power) was exposed. It is observed that there are two undesirable hotspots near the slot apertures and the field from each slot are combined at the central region of the spherical phantom. In application the desirable hotspot is only in the central one and the other two hotspots closes to the slots should be eliminated. When a cold water bolus (12–14°C), of which the shape is concentric spherical plastic bag with 2 mm seperation was employed using the water flow rate of 0.5 l/min, the two undersirable hotspots could be removed. There remains only a desirable hotspot which EFS is 1.0 cm^2 and penetration depth is 2.5 cm at the central region of the spherical phantom as shown in Fig. 9(b). This experimental result implies that when an appropriate cold water bolus is applied, this applicator can be used to perform local heating in the spherical part of a human body efficiently.

For a planar phantom experiment, Fig. 10 shows the dimensions of the phantom and water bolus incorporated with the measuring planes. Thermographs of a four-slot applicator with the net power of 119 W is shown in Fig. 11. Fig. 11(a)

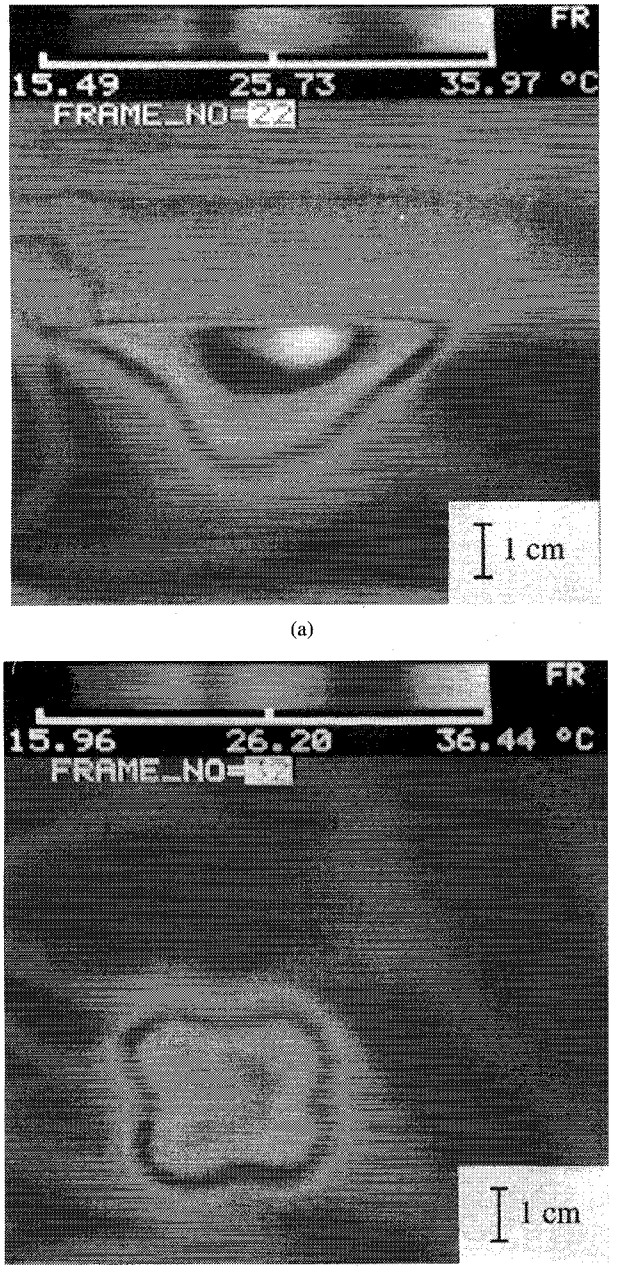

Fig. 11. Heating pattern of a four-slot applicator in a flat phantom. (a) Vertical plane pattern. (b) Horizontal plane pattern.

shows the heating pattern on the vertical plane which implies that the penetration depth is about 3 cm. The heating pattern on the horizontal plane which is 2 cm from the surface is shown in Fig. 11(b). On this plane from this figure, the EFS is about 13.8 cm^2 and it looks like a rectangle where the vertices are in the direction of each slot. It is evident that the size and shape of the hotspots can be varied by using different number of slot. The more the number of slots, the larger the size of the hotspot. This results from the reason that the slot lengths are decreased as the number of slots are increased. It is also observed that the maximum temperature rise is increased as the number of slots is increased. Moreover it is noted that the maximum heating depth is about 3 cm. It is deeper than a conventional open waveguide counterpart which the maximum depth is always limited to a skin depth about 1.7 cm [12].

It is recommended that applicators intended for therapy should be capable of producing SAR values of 235 W/kg in the muscle region [23]. From the experimental results of heating patterns mentioned above, we can calculate the net input power required for obtaining that value in the muscle region by measuring $(dT/dt)|_{t=0}$ from (5). The input powers are illustrated in Table II. It is seen that the input power becomes lower by increasing a number of the slot.

V. Conclusions

The design and development of a spherical slot array applicator for a microwave local hyperthermia are described. The induced SAR distribution inside the tissues is analyzed, and the theoretical results are found to be in a good agreement with field mapping and thermographic measurements in phantoms. The spherical slot array applicator offers the advantage of being lightweight, rugged, easy to handle and useful for heating part of a spherical shape such as a breast. It is possible to heat tumors selectively with small size (about 1 cm in diameter). A satisfactory power penetration depth of 3 cm is achieved. These results show that the heating depth can be increased by a factor of 1.8 over that obtained from conventional waveguide applicators of which the depth of heating is approximately 1.7 cm at this frequency. Cooling of the skin is accomplished by using a cooling water bolus of which the shape is conformed to the applicator and tissue surfaces. One way to vary the heating volume is accomplished by using different number of slots. For the larger spherical part such as head, dimensionally scaled applicator at lower frequency can be designed using the principles described.

Acknowledgment

The authors deeply appreciate Mr. K. Hiraguri, JICA expert, for his support throughout the project.

References

[1] I. J. Bahl, S. S. Stuchly, and M. A. Stuchly, "A new microstrip radiator for medical applications," *IEEE Trans. Microwave Theory Tech* ., vol. MTT-28, no. 12, pp. 1461–1468, Dec. 1980.

[2] M. A. Stuchly, S. S. Stuchly, and G. Kantor, "Diathermy applicators with circular aperture and corrugated flange," *IEEE Trans. Microwave Theory Tech.*, vol. MTT-28, no. 3, pp. 267–271, Mar. 1980.

[3] I. J. Bahl, S. S. Stuchly, and M. A. Stuchly, "New microstrip slot radiator for medical applications," *Electron Lett* , vol. 16, no. 19, pp. 731–732, Sept. 1980.

[4] Y. X. Wang, "Slot-line coupler for medical applications," *Electron Lett.*, vol. 20, no. 22, pp. 939–940, Oct. 1984.

[5] R. H. Johnson, "New type of compact electromagnetic applicator for hyperthermia in the treatment of cancer," *Electron Lett* ., vol. 22, no. 11, pp. 591–593, May 1986.

[6] R. Leedee, M. Chive, and M. Plancot, "Microstrip microslot antennas for biomedical applications: Frequency analysis of different parameters of this type of applicator," *Electron Lett.*, vol. 21, no. 7, pp. 304–305, Mar. 1986.

[7] N. K. Vzunoglu, E. A. Angelikas, and P. A. Cosmidis, "A 432-MHz local hyperthermia system using an indirectly cool, water-loaded waveguide applicator," *IEEE Trans. Microwave Theory Tech* ., vol. MTT-35, no. 2, pp. 106–111, Feb. 1987.

[8] J. Loane, H. Ling, B. F. Wang, and S. W. Lee, "Experimental investigation of a retro-focusing microwave hyperthermia applicator:

Conjugate-field matching scheme," *IEEE Trans. Microwave Theory Tech.*, vol. MTT-34, no. 5, pp. 490–494, May 1986.
[9] J. W. Hand, J. L. Cheetham, and A. J. Hind, "Absorbed power distributions from coherent microwave arrays for localized hyperthermia," *IEEE Trans. Microwave Theory Tech* ., vol. MTT-34, no. 5, pp. 484–489, May 1986.
[10] W. Gee, S. W. Lee, N. K. Bong, C. A. Cain, R. Mittra, and R. L. Magin, "Focused array hyperthermia applicator: Theory and experiment," *IEEE Trans. Biomedical Engineering*, vol. BME-31, no. 1, pp. 38–46, Jan. 1984.
[11] J. R. James, C. M. Hall, and G. Andrasic, "Angled dual compact hyperthermia applicators," *IEE Proc.*, vol. 134, Pt. H, no. 3, pp. 315–320, June 1987.
[12] Y. Nikawa, H. Watanabe, M. Kikuchi, and S. Mori, "A direct-contact microwave lens applicator with a microcomputer-controlled heating system for local hyperthermia," *IEEE Trans. Microwave Theory Tech.*, vol. MTT-34, no. 5, pp. 626–630, May 1986.
[13] Y. Nikawa, T. Katsumata, M. Kikuchi, and S. Mori, "An electric field converging applicator with heating pattern controller for microwave hyperthermia," *IEEE Trans. Microwave Theory Tech.*, vol. MTT-34, no. 5, pp. 631–635, May 1986.
[14] Y. Nikawa and F. Okada, "Dielectric-loaded lens applicator for microwave hyperthermia," *IEEE Trans. Microwave Theory Tech.*, vol. 39, no. 7, pp. 1173–1178, July 1991.
[15] A. W. Guy, C. K. Chou, and K. H. Luk, "915-MHz phased array system for treating tumors in cylindrical structures," *IEEE Trans. Microwave Theory Tech.*, vol. MTT-34, no. 5, pp. 502–507, May 1986.
[16] M. Krairiksh, T. Wakabayashi, and W. Kiranon, "Characteristics of microwave applicator using slots on a sphere," *Med. and Biol. Eng. and Comp.*, vol. 29, suppl. part 1, p. 425, 1991.
[17] M. Krairiksh, T. Wakabayashi, and W. Kiranon, "Microwave applicator using two slots on sphere," in *Proc. Fourth Asia-Pacific Microwave Conf.*, Adelaide, Australia, 1992, pp. 225–228.
[18] S. A. Schelkunoff, *Electromagnetic Waves*. D. Van Nostrand, 1943, ch. 10.
[19] M. Krairiksh, T. Wakabayashi, and W. Kiranon, "Analysis of interior electromagnetic fields from a slot on a perfectly conducting sphere," in *Proc. Third Asia-Pacific Microwave Conf.*, Tokyo, 1990, pp. 1183–1186.
[20] A. W. Guy, "Analysis of electromagnetic fields induced in biological tissues by thermographic studies on equivalent phantom models," *IEEE Trans. Microwave Theory Tech.*, vol. MTT-19, pp. 205–214, Feb. 1971.
[21] M. V. Prior, M. L. D. Loumori, G. R. Forse, and J. W. Hand, "Current sheet applicator arrays for superficial hyperthermia: Incoherent versus coherent operation," *Medical and Biological Engineering and Computing*, vol. 29, suppl. part 1, p. 425, 1991.
[22] G. Gajda, M. A. Stuchly, and S. S. Stuchly, "Mapping of the near-field pattern in simulated biological tissues," *Electron Lett.*, vol. 15, no. 4, pp. 120–121, Feb. 1979.
[23] R. H. Johnson, J. R. James, J. W. Hand, J. W. Hopewell, P. R. C. Dunlop, and R. J. Dickinson, "New low-profile applicators for local heating of tissues," *IEEE Trans. Biomed. Eng.*, vol. BME-31, no. 1, Jan. 1984.

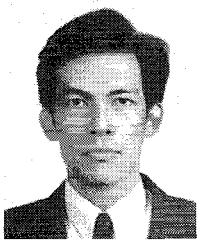

Monai Krairiksh was born in Bangkok, Thailand, on June 19, 1957. He received the B.Eng and M.Eng degrees from King Mongkut's Institute of Technology, Ladkrabang, Bangkok, Thailand, in 1981 and 1984, respectively.

In 1981, he joined the staff of King Mongkut's Institute of Technology, Ladkrabang and is presently an assistant professor. Since 1988, he has been involved with development of microwave applicators for medical and industrial applications.

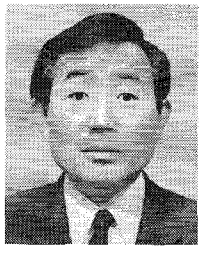

Toshio Wakabayashi (S'68–M'70) was born in Tochigi, Japan, on May 4, 1945. He received the B.E. and M.E. degrees from Tokai University, in 1968 and 1970, respectively. He received the D.E. degree from the same university in 1985.

In 1970 he joined Faculty of Engineering, Tokai University, and since then, as a faculty member he has engaged in research in the field of electromagnetic waves, including fields in dielectric and optical waveguides, and microwave hyperthermia. Since 1988 he has been a professor in the Department of Communication Engineering. He was a visiting researcher in the Department of Electrical Engineering, University of California, Los Angeles (UCLA) in 1991.

Dr. Wakabayashi is a member of the IEICE, Japan and the Japanese Cancer Association.

Wiwat Kiranon received the B.Eng degree in electrical engineering from King Mongkut's Institute of Technology Ladkrabang, Bangkok, Thailand, in 1972 and the M.Eng and D.Eng degrees from Tokai University, Japan, in 1975 and 1983, respectively.

He is presently an associate professor in the Telecommunication Engineering Department at King Mongkut's Institute of Technology Ladkrabang, Bangkok, Thailand. His research interests are in the areas of analog circuits, signal processing, and various aspects of applications in instrumentation problems.